Journal of Statistical Physics, Vol. 105, Nos. 3/4, November 2001 (© 2001)

Iterated Fully Coordinated Percolation on a Square Lattice

E. Cuansing and H. Nakanishi[1]

Received February 13, 2001; revised May 11, 2001

We study, on a square lattice, an extension to fully coordinated percolation which we call iterated fully coordinated percolation. In fully coordinated percolation, sites become occupied if all four of its nearest neighbors are also occupied. Repeating this site selection process again yields the iterated fully coordinated percolation model. Our results show a large enhancement in the size of highly connected regions after each iteration (from ordinary to fully coordinated and then to iterated fully coordinated percolation); enhancements that are much larger than an extension of correlations by an extra lattice constant might suggest. We also study the universality among the three problems by determining the corresponding static and dynamic critical exponents. Specifically, a new method to directly calculate the walk dimension, d_w, using finite size scaling applied to normal mode analysis is used. This method is applicable to any geometry and requires significantly less computation than previously known calculations to determine d_w.

KEY WORDS: Percolation; critical exponents; scaling laws.

1. INTRODUCTION

Iterated fully coordinated percolation (referred to as IFC percolation from this point on) is an extension to the ordinary percolation and the *fully coordinated percolation* (referred to as FC percolation hereon) models. Ordinary percolation is a well-known problem of geometrical phase transition where the global connectivity is singular as a function of the local connectivity (see, for a review, Stauffer and Aharony[1]). In ordinary site

[1] Department of Physics, Purdue University, West Lafayette, Indiana 47907; e-mail: cuansing@physics.purdue.edu

0022-4715/01/1100-0659$19.50/0

percolation on a lattice, sites are randomly occupied with an independent occupation probability p. Two nearest neighbor sites are considered connected if they are both occupied. A collection of connected sites, i.e., every site in the group is connected to every other site either directly or through paths of nearest neighbors, is termed a cluster. When p is increased until it reaches a critical value p_c, an infinitely spanning cluster will form for the first time. The square lattice shown in Fig. 1a is an example of ordinary site percolation on a square lattice. Occupied sites are shown as circles while unoccupied sites are not shown.

To perform IFC percolation, first perform ordinary percolation. After this is done, determine which of the occupied sites have all four of their nearest neighbors also occupied. Occupied sites having this property are called *fully coordinated sites* and will remain occupied while the other sites will be removed. This process of winnowing occupied sites was described in ref. 2 and we called the resulting model the *fully coordinated percolation* model (FC percolation). The square lattice shown in Fig. 1b is an example of fully coordinated percolation constructed from the ordinary percolation sites shown in Fig. 1a. The gray-filled circles are fully coordinated sites. The final step in the process is to again choose fully coordinated sites but this time from the resulting system constructed from FC percolation. As in the FC percolation case, we also remove the sites that are not fully coordinated. The solid circles in the square lattice shown in Fig. 1c are examples of IFC percolation sites constructed from Figs. 1a and 1b.

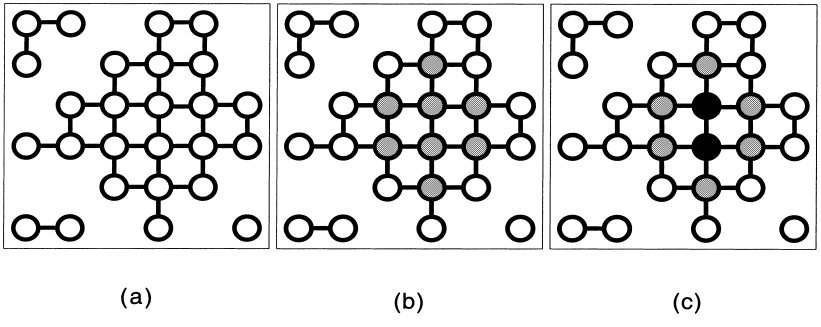

Fig. 1. An illustration of the process to simulate IFC percolation. (a) First we simulate ordinary percolation on a square lattice. Occupied sites are shown as circles while unoccupied sites are not shown. (b) From the resulting sites from ordinary percolation, choose the fully coordinated sites, i.e., occupied sites whose four neighbors are also occupied. These sites are shown as gray-filled circles. (c) Repeat the culling of non-fully coordinated sites one more time. The remaining sites are then considered as sites in IFC percolation. These sites are shown as solid circles in the figure.

Notice that this problem is different from bootstrap percolation (see, for a review, Adler[3]) where sites of less connectivity are iteratively removed until no more sites have insufficient connectivities. In our problem, we only perform the culling of non-fully coordinated sites twice. Another closely related problem is the so-called high-density site percolation problem[4] wherein sites with a minimum number m of occupied neighbors are retained and the rest are culled. If $m = z$ in the high density percolation problem where z is the full lattice coordination number, then it is the same as FC percolation. This class of problems (including essentially similar bond percolation problems[5]) were studied by various methods previously for their static critical behavior. However, to our knowledge, our previous work[2] was the first to study the dynamic critical exponents, and the current work is the first to study the IFC extension of the problem.

A physical example where FC percolation may be relevant is the behavior of supercooled water where the hydrogen bonds forming a 4-coordinated ice structure play important roles.[5] High density percolation is generally thought to be relevant to a large class of problems. To mention just one recent example of such a system, Yb in an alloy $YbCu_2Si_2$ where Ni is randomly substituted for Cu becomes magnetic only when it has at least two neighboring Ni ions. Thus, as the Ni concentration is varied, the system undergoes a phase transition.[6] There are many more examples of systems where magnetic or electric properties of a constituent depends on its local environment.[7–10]

IFC percolation is an example of a problem which interpolates between high density and bootstrap percolation. The basis of bootstrapping was the need to self-consistently *qualify* sites with regard to a requirement on their local environment in terms of likewise *qualified* neighbors. If instead the local environment requirement is multi-fold but not self-consistently bootstrapping, one arrives at a finite level of culling as in IFC percolation. For example, consider a random alloy where the requirement for an ion to be magnetic is: (1) it must have certain number of *qualified* helpers as neighbors, and (2) an ion is qualified as a helper if it has a certain number of A ions as neighbors. Note that the second requirement does not bootstrap as it does not require magnetic neighbors. Another theoretically possible scenario is in layered adsorption. Consider the following situation: a surface adsorbed atom sticks only if a certain number of neighboring sites also have adsorbed atoms (otherwise desorbing), and only the high density adsorbed region serves as the substrate onto which the next layer can adsorb. Note that in the first scenario of magnetic alloys, *culling* does not mean the actual removal of nonmagnetic ions while in the second example of adsorption, actual desorption of adsorbate atoms takes place.[11]

In our earlier work,[2] we found that the sizes of the fully-connected subregions (with no internal holes) in an incipient infinite cluster in FC percolation are much larger than those found in ordinary percolation. In this study, we find the rapid increase in the sizes of the fully-connected subregions to continue when the full coordination requirement is iterated one more time. The regions of high local connectivity are generally interesting because they would seriously affect such dynamic problems as diffusion constrained to occur on the cluster and the vibrational modes in an equivalent disordered network of *springs*. In particular, it was found previously that they enter into the scaling of the normal mode spectrum.[12]

In the same previous work,[2] we also concluded that the dynamic critical exponents of FC percolation were close to but different from those of ordinary percolation, drawing this conclusion from numerical results on FC percolation clusters which were grown from a seed site until prescribed sizes were reached. The verification of this result when clusters are instead generated on a square grid of fixed size was one of the motivations of this work. The main motivation, however, was to extend our studies to the iterated model; the original questions of which included whether the universality change suggested in ref. 2 would continue when the full coordination constraint is iterated, perhaps approaching a limit (possibly a unique, high-connectivity limit similar to the case for the loop-enhanced percolation problem.[13])

In this work we obtain numerical results on the corresponding dynamical critical exponents of FC and IFC percolation from the clusters generated statically on square grids of prescribed sizes. In contrast to ref. 2, our new results indicate that the numerical values of these exponents are the same within the aggregate error bounds for ordinary and FC percolation, and the same is true even for the new IFC extension. Since the actual numerical estimates for the FC problem from this work and the previous one are compatible within their error estimates, this might simply mean that we drew an overzealous conclusion in our previous work as far as FC percolation. However, we cannot rule out the possibility that the ensembles of clusters used in ref. 2 and the current work may contain subtle differences which consequently alter dynamic universality classes. Further discussions on this subtlety can be found in Section 4.

The rest of this paper is divided into four sections. In Section 2 we present numerical results and calculations of the static and dynamic critical exponents of IFC percolation. The geometry of clusters is studied in Section 3 with a particular focus on the sizes and distributions of the highly connected subregions. The difference between the methods of generating the cluster ensemble in ref. 2 and the current work is discussed in Section 4. The final section gives a summary of our results.

2. STATIC AND DYNAMIC CRITICAL BEHAVIOR

We have determined the static and dynamic critical exponents of IFC percolation by simulations on a square grid. The culling of non-fully coordinated sites occurs in two stages. After sites in the grid are randomly occupied with an independent probability p, all the fully coordinated sites are marked. After this marking process is done, all the occupied but unmarked sites are removed. From the resulting system of remaining sites, we again determine which sites are fully coordinated and remove those which are not. Figures 1a–1c depict this process. To determine the connectivities among the sites, we have used the standard Hoshen–Kopelman algorithm.[14]

The critical occupation probability, p_c, is determined from the plot of susceptibility, χ, against p. This plot is shown in Fig. 2. Notice that because of finite size effects, instead of a diverging χ at p_c, we see clearly defined peaks at p values near the true p_c. The lattice sizes, L^2, we used in our simulations were $L = 256$, 512, 1024, and 2048, and each data point in Fig. 2 is an average over 1000 realizations. According to the plot, the susceptibility peaks are pegged at $p_{\text{peak}} = 0.946$ for the larger lattices. Since the larger the lattices the more our simulations mimic the asymptotic limit, we

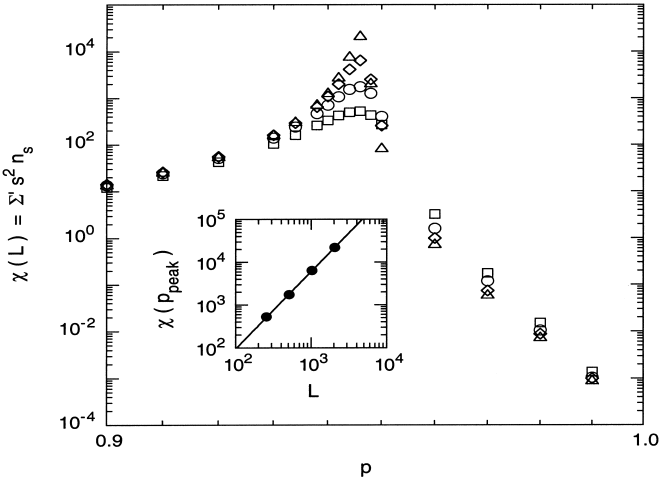

Fig. 2. Susceptibilities χ against probability p in IFC percolation on square lattices of sizes L^2 are shown. The squares, circles, diamonds, and triangles are for $L = 256$, 512, 1024, and 2048, respectively. Each data point in the plot is an average over 1000 realizations. Shown as the inset is the finite-size scaling of the susceptibility peaks by plotting the four peaks against L on a log–log scale. Note that L is a dimensionless quantity corresponding to the length, in multiples of the lattice constant, of the side of the square lattice.

can conservatively assign the value for the critical occupation probability to be at $p_c = 0.946 \pm 0.001$.

The ratio between critical exponents γ and ν can be determined from the scaling of susceptibility peak values against the corresponding lattice sizes, i.e., $\chi(p_{peak}, L) \sim L^{\gamma/\nu}$. Using this relationship we find γ/ν for IFC percolation to be 1.805 ± 0.018. This value agrees with the value for ordinary percolation which is known exactly to be $43/24 \approx 1.7917$. The ratio γ/ν can also be used to indirectly determine the fractal dimension, d_f, from the known scaling relationship, $d_f = 1 + \gamma/2\nu$. The result for IFC percolation is $d_f = 1.903 \pm 0.009$ while the known exact value for ordinary percolation is $91/48 \approx 1.8958$. The critical exponent γ can also be determined independently from the scaling of susceptibility against the occupation probability p, which goes as $\chi(p, L = \infty) \sim |p - p_c|^{-\gamma}$, where the $L = \infty$ indicates the scaling to be ideally satisfied in the asymptotic limit of $L \to \infty$. As in the case of FC percolation, the susceptibility peaks are very close to $p = 1.0$. This provides data to the right of the peaks to reside in a small interval. We therefore only use data to the left of the peaks to determine the scaling implied. The value we found for γ in IFC percolation using $p_c = 0.946$ is $\gamma = 2.398 \pm 0.039$. This value also agrees very well with the value in ordinary percolation, known to be exactly $43/18 \approx 2.3889$.

The fractal dimension, d_f, of IFC percolation can also be determined directly. At p_c, the size of the largest cluster, S, scales with L as $S \sim L^{d_f}$, where $d_f = 1.857 \pm 0.007$. This value is close to the known exact value for ordinary percolation as well as to the value obtainable from our measured γ/ν.

Listed in Table I are the values for the ratio γ/ν and for d_f we found from our simulations of ordinary, FC, and IFC percolation. As a reference, the previously determined values of the corresponding critical exponents for ordinary percolation are listed at the bottom row of the table.

Table I. The Ratio Between Static Critical Exponents γ and ν, and the Fractal Dimension d_f Found for Ordinary, FC, and IFC Percolation Models Are Shown. The Values at the Bottom Row of the Table Are Previously Determined Values for Ordinary Percolation. The γ/ν Ratio for Ordinary Percolation Is Not Determined in this Work

percolation type	γ/ν	fractal dimension, d_f
ordinary	—	1.888 ± 0.004
FC	1.791 ± 0.006	1.885 ± 0.014
IFC	1.805 ± 0.018	1.857 ± 0.007
ordinary (prior results)	$\frac{43}{24}$ (≈ 1.7917)[a]	$\frac{91}{48}$ (≈ 1.8958)[a]

[a] See, e.g., Stauffer and Aharony.[1]

The values for the spectral dimension, d_s, and the walk dimension, d_w, can be determined from the dynamic critical behavior of IFC percolation. We first construct the transition probability matrix **W**. The elements, W_{ij}, of this matrix are the hopping probabilities per step of a random walker to hop from site j to site i. The diagonal elements W_{ii} are the probabilities for the walker to stay at site i for a time step. In the *myopic ant* rule, all of the W_{ii} are zero. In contrast, in the *blind ant* rule, the W_{ii} may be nonzero, their values dependent on how many occupied neighboring sites the walker can hop into (see, for a review, ref. 16). We are using the blind ant rule for this work.

Once the **W** matrix is determined, the value of d_w can be estimated directly from its largest non-trivial eigenvalue, λ_1. This eigenvalue satisfies the finite size scaling law[17]

$$|\ln\ \lambda_1| \approx 1-\lambda_1 \sim S^{-2/d_s}. \tag{1}$$

For our simulations, the lattice size L is fixed but the cluster size S fluctuates. Thus it is most convenient to express this in terms of L instead of S. Making use of the Alexander–Orbach scaling law,[18] $d_s = 2d_f/d_w$, and $S \sim L^{d_f}$, we obtain

$$1-\lambda_1 \sim L^{-d_w}. \tag{2}$$

There are several ways of estimating d_w. One method is to obtain the mean square displacement of a random walk by numerically iterating the **W** matrix and then using the method of successive slopes to determine the exponent.[15] Another method is to use spectral analysis to evaluate the velocity auto-correlation function; a method wherein detailed knowledge of the eigenvectors of **W** is required (see, for a review, ref. 16). Using Eq. (2) on the other hand requires only that we determine the average of the first nontrivial eigenvalue λ_1 for each value of the lattice size L and does not rely on values or estimates of any other exponents. This route of estimating d_w is computationally simpler than the two other methods mentioned and is applicable for any geometry.

Shown in Fig. 3 is our data plotted in a way that is consistent with Eq. (2). For each percolation type, we used 13 different edge lengths of the square lattices that range from $L = 94$ to $L = 198$. Furthermore, for each data point, about 1000 random realizations of the **W** matrix had been generated by Monte Carlo simulations. To numerically determine λ_1 from each **W** matrix, we used the *Arnoldi–Saad* method.[20]

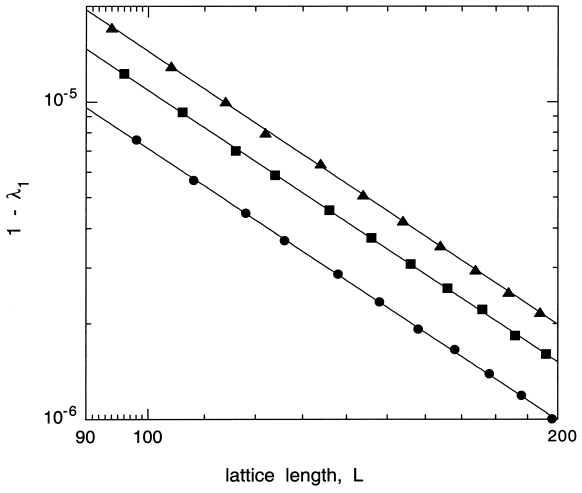

Fig. 3. Shown is the scaling of the largest nontrivial eigenvalue λ_1 by plotting $1-\lambda_1$ against the lattice length L on a log–log scale. The circles, squares and triangles are for ordinary, FC, and IFC percolation, respectively. Each data point in the plot is an average over 1000 random realizations.

Listed in the second column of Table II are the d_w values we found following Eq. (2) for ordinary, FC and IFC percolation. Notice that there is an excellent agreement among the values for all three cases and that they agree with the previously known value for ordinary percolation.

In the third column of Table II are listed the d_s values calculated using the Alexander–Orbach scaling law. Although all three estimates from this work agree with the previously known value for ordinary percolation within

Table II. Shown Are the Walk and Spectral Dimensions for Ordinary, FC, and IFC Percolation. The Walk Dimensions Were Determined by Taking the Largest Non-Trivial Eigenvalue of W While the Spectral Dimensions Are Derived from $d_s=2d_f/d_w$, with d_f Values Taken from Table I. The Last Row in the Table Contains Previously Known Values for Ordinary Percolation

percolation type	walk dimension, d_w	spectral dimension, d_s
ordinary	2.841 ± 0.015	1.329 ± 0.010
FC	2.843 ± 0.015	1.326 ± 0.017
IFC	2.857 ± 0.015	1.300 ± 0.012
ordinary (prior results)	2.87 ± 0.02[a]	1.30 ± 0.02[b]

[a] See Majid *et al.*[7]
[b] See, e.g., Nakanishi.[8]

the aggregate error estimates of our work and those of the previous work, there is a slight internal discrepancy between our own estimate of d_s for ordinary percolation and that for IFC percolation. Since d_s is derived from d_f and d_w, the slight discrepancy may be attributed to the d_f value we found for IFC percolation by direct simulation (refer to the third column of Table I). We suspect an unaccounted systematic error occuring when we perform each iteration process. In particular, as we will discuss in more detail later, the length scales associated with fully-coordinated subregions appear to increase at each iteration. This suggests that we may have to increase the overall lattice length scale correspondingly in order to maintain a good estimate of the fractal dimension by direct simulation. Since this was not done in this work, a systematic error may have crept in this way.

3. GEOMETRY OF CLUSTERS

Previously,[2] it was found that the number of *interior* sites in the largest cluster in FC percolation is much greater than that in ordinary percolation at their respective thresholds. In this work we find that this trend continues further for IFC percolation. As an illustration, consider Figs. 4a and 4b. Shown in Fig. 4a is the largest cluster from a simulation of ordinary percolation on a 200×200 square lattice at its percolation threshold. The darker dotted sites are *fully-coordinated* (FC) sites while the lighter gray dotted sites are *partially-coordinated* (PC) sites. FC sites are those all of whose neighbors are also occupied (thus these are similar to, though not identical with, the *interior* sites considered in ref. 2), while PC sites have at least one nearest neighbor not occupied. The same shading tone is used in Fig. 4b except that what is shown is the largest cluster from a simulation of IFC percolation at its own percolation threshold. Notice the difference in the number of FC sites in these figures. Partially coordinated sites dominate in ordinary percolation while FC sites dominate in IFC percolation.

The average number of FC and PC sites in ordinary, FC, and IFC percolation are plotted in Fig. 5. Linear least squares fits indicate that in ordinary percolation the PC sites are more than 6 times as many as the FC sites, while the ratio in FC percolation is about 1.5, and in IFC percolation it is only about 0.86. A trend that can easily be seen here is that the number of FC sites increases as we progress from ordinary to FC and then to IFC percolation. Although only a local full-coordination correlation is imposed, it clearly results in a change on the global scale. This may be reflected in some qualitative differences in a physical property if it is sensitive to the size of connected clusters of FC sites. For example, if a percolation model

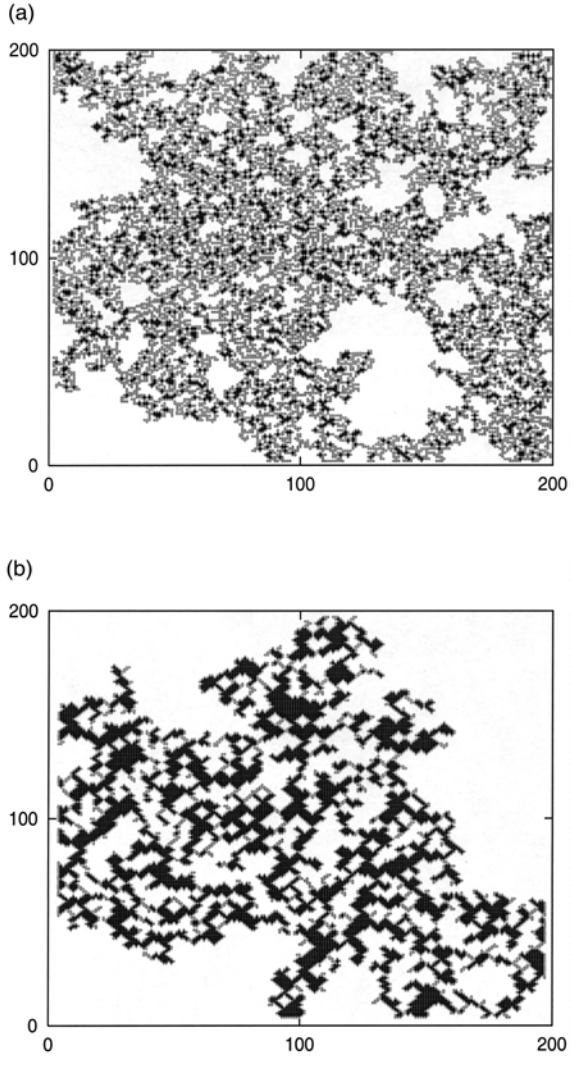

Fig. 4. Sample largest clusters resulting from simulating ordinary and IFC percolation at their respective percolation thresholds in a 200×200 square lattice with free boundaries are shown. The darker dotted sites are FC (fully coordinated) sites while the lighter gray dotted sites are PC (partially coordinated) sites. (a) For ordinary percolation, PC sites dominate. The occasional FC sites are clumped together and are somewhat distributed evenly in the cluster. (b) For IFC percolation, the number of FC sites increases.

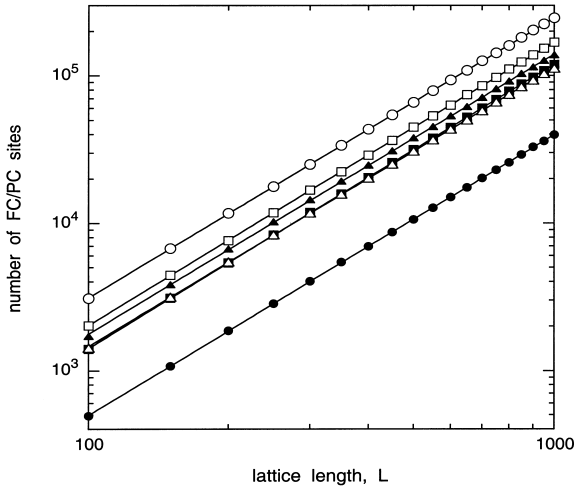

Fig. 5. A log–log plot of the number of FC and PC sites in the largest cluster at the percolation threshold against the lattice length L is shown. The circles are for PC sites while the solid circles are for FC sites, both in ordinary percolation. The data points for FC percolation are the squares (which are for PC sites) and the solid squares (which are for FC sites). For IFC percolation, the triangles are for PC sites while the solid triangles are for FC sites. Each data point is an average over 2000 random realizations.

is used to describe a disordered substrate on which diffusive physics takes place (such as in catalysis), what is expected within a given time scale (or frequency range) would be directly affected by the size of the high-connectivity or FC regions of the substrate where a more transient kind of diffusion occurs compared to less well connected areas. In such cases, it is expected that there would be large differences depending on whether the appropriate percolation model to use is ordinary, FC, or IFC percolation. The latter cases could be a better representation if the culling of partially coordinated sites naturally occurs in the particular problem, say, due to desorption.[11]

The distribution of cluster sizes (of all sites, i.e., both FC and PC sites) is shown in Fig. 6. Because of the finite size effects, only the intermediate size ranges (about 10^2 to 10^4 site clusters) are consistent with the cluster size scaling $N_s \sim s^{-\tau}$ with the ordinary percolation value of $\tau = 187/91 \approx 2.055$, where s is the cluster size and N_s is the number of clusters having size s. Very small s values are clearly out of the asymptotic scaling regime while the scaling region where $s \sim \mathcal{O}(L^{d_f})$ is also limited by the finite size of the grid. Nonetheless, it is important to note that there is no significant difference between ordinary, FC, and IFC percolation for all

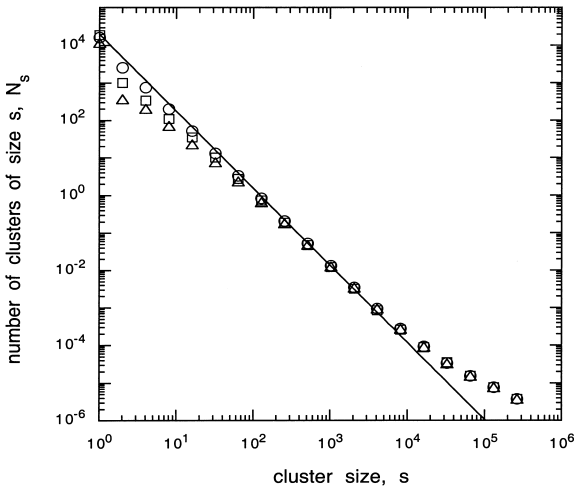

Fig. 6. A distribution of cluster sizes is shown in a log–log plot. The circles, squares and triangles are for ordinary, FC, and IFC percolation, respectively. Each data point is an average over 2000 random realizations. The line drawn is not the best fitting line but instead one that follows $N_s \sim s^{-\tau}$.

s above about 10^2. This suggests strongly that the asymptotic cluster size scaling (which is known to occur for ordinary percolation) also occurs for both FC and IFC percolation.

In making the plot for Fig. 6, we didn't distinguish between PC and FC sites in the clusters. If we instead just consider FC sites and make a semi-log plot of the number of clusters formed by these sites against the corresponding cluster sizes, we should be able to roughly estimate the characteristic cluster sizes formed by FC sites alone. Shown in Fig. 7a is N_s against s of clusters formed by FC sites in ordinary percolation. The line shown is not a best fitting line for all of the available points but instead one that best fits only the four middle points and is shown merely to obtain a crude idea of the typical size scale of FC clusters. For ordinary percolation, we found the typical FC cluster size to be around $s_0 \approx 2$ FC sites. Shown in Figs. 7b and 7c are data for FC and IFC percolation, respectively. We found that around $s_1 \approx 18$ FC sites comprise the average cluster in FC percolation while around $s_2 \approx 72$ FC sites make up the average FC cluster in IFC percolation. This means that in order to map the FC and IFC percolation problems to the same length scale as ordinary percolation, a length rescaling by $\sqrt{s_1/s_0} \approx 3$ and $\sqrt{s_2/s_0} \approx 6$ must be performed, respectively. Thus, although both static and dynamic critical exponents seem to remain the same as the full coordination rules are iteratively applied, the local

connectivity greatly changes or, equivalently, the length scale which would approximately preserve the local connectivity changes by factors which are larger than an extension of correlations by a lattice constant might suggest. It should also be noted that the implementation of the full coordination constraint results in a discrete change of the problems and thus the above length rescaling is not expected to map FC or IFC percolation clusters to the ordinary percolation clusters *exactly* as an infinitesimal rescaling might. Neither is it expected that the rescaling factor from IFC to FC be identical to that from FC to ordinary percolation.

4. COMPARISON WITH PREVIOUS WORK ON FC PERCOLATION

In this work, we follow the prescription described in the Introduction closely in order to generate the ensemble of FC and then IFC clusters. The only limitation in the Monte Carlo portion of our work are that the grid we use to generate the clusters must be finite and that a particular boundary condition must be selected. Our largest grid is 2048×2048 and clearly, this is not very large by today's standards. Since we use finite size scaling in the determination of both the static and dynamic critical exponents, the finiteness of the grid (and cluster) is in fact necessary; yet, there is always a possibility that an asymptotic regime of large sizes may not have been reached. Also, we use the free boundary condition with no direct connectivity across the opposite edges of the grid, which may accentuate the finite size limitations. This type of ensemble is the most straightforward extension of the standard Monte Carlo simulation of ordinary percolation to the FC and IFC percolation models, and may be described as *static* since there is no dependence on the order in which sites are generated or the connectivities checked. Indeed, the static exponents γ, γ/ν, and the like, agree closely with the corresponding ordinary static percolation values, and, if the length scale is identified with the grid edge length, then the cluster's fractal dimensions should also agree closely with that of ordinary percolation.

In our previous work,[2] we studied the static and dynamic critical behavior of FC percolation using the ensemble of clusters of specified number of sites, say, S'. Those clusters were grown from a seed site by applying a *breadth-first* algorithm twice; i.e., first generating an ordinary percolation cluster in nearest neighbor shells to a sufficiently large size (say, $5S'$), and then identifying and joining only the fully coordinated sites in a second *searching* process from the same seed and then stopping the process when the size of the resulting connected cluster reaches the predetermined value S'. Now, if we make the intermediate cluster of the first search process very large and if we do *not* terminate the second search process arbitrarily when S' is reached, but rather continue the search until the

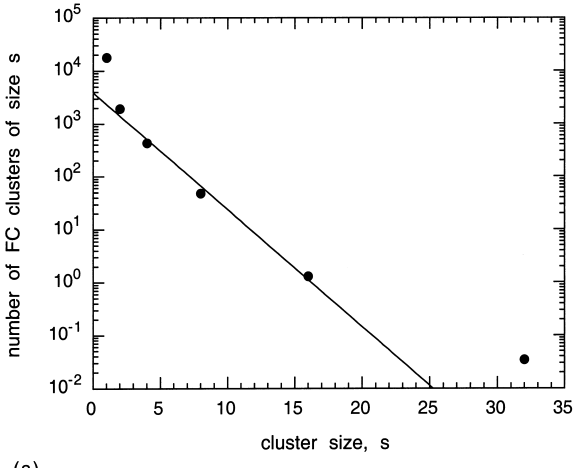

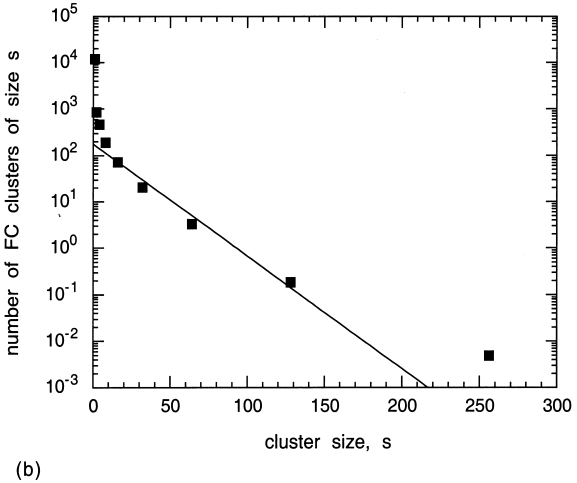

Fig. 7. Shown are semi-log plots for the number of clusters formed by FC sites against the corresponding cluster sizes. Each line drawn in each plot does not correspond to the best fit line for all available points but only for the four middle points. This would give a rough estimate of the average FC cluster sizes. (a) In ordinary percolation, on average there are 2 FC sites in each FC cluster. (b) In FC percolation, on average FC clusters have 18 FC sites. (c) In IFC percolation, there are around 72 FC sites in an FC cluster.

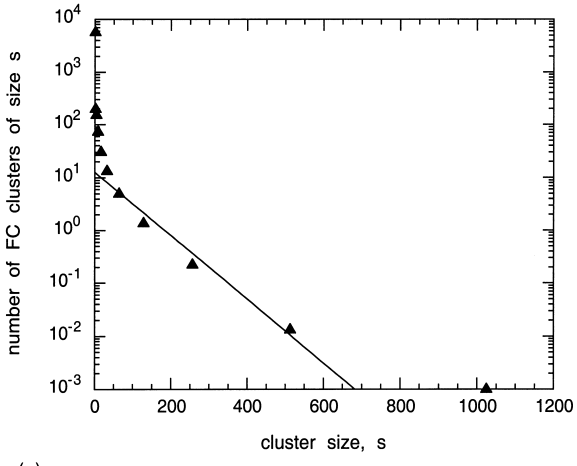

Fig. 7. (Continued).

natural boundary of the FC cluster is found, then the resulting cluster ensemble should be *exactly* the same as that which would result in the *static* ensemble of FC percolation clusters generated on an *infinite* grid. However, since the first stage is stopped at $\leqslant 5S'$ and since the second stage is forcibly stopped exactly at S', which is a predefined value, we introduced a kinetic nature to the cluster ensemble. This may be somewhat similar to the differences in the degree of intrinsic anisotropy in static and *kinetic* ensembles of percolation clusters studied previously[21, 22] (called *equlibrium* versus *growing* clusters there).

An illustration of the cluster geometry differences arising between a static cluster and a growing one is shown in Fig. 8. In the static ensemble, every site of the spanning, connected component of the ordinary, FC, or IFC percolation models' realizations within a given length scale L (defined to be the grid edge length) is a part of the cluster. In the growing cluster, on the other hand, only those sites which are within a certain path length along the nearest neighbor connections from the seed site are counted, independent of how close they are by straight line distance to the seed. Also, since cluster size S' is the control parameter for this ensemble, the length scale L is not precisely fixed but rather obtained as an average for a given value of S'. Exactly which sites are counted in a cluster of length scale L and which ones excluded do clearly depend on the particular search order that is employed. Thus, typically, for the same L, the number of sites of the percolating cluster is smaller in the growing cluster ensemble than in

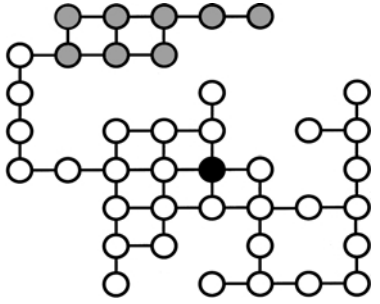

Fig. 8. Figure to illustrate cluster geometry differences between growing a cluster from a seed and generating it in a square lattice (static ensemble). The solid circle is the seed and the cluster grown from it includes all the circles but excluding the gray-filled ones. The growth process stops when a specified cluster size is reached. In this figure, the gray-filled circles are excluded because the specified cluster size has already been reached; however, when generating the cluster in a square lattice of the same length scale, the gray-filled circles will be included in the cluster.

the static one. This tends to reduce both the fractal dimension d_f and the walk dimension d_w estimates. If the effect is more pronounced for d_w, then it may explain why an apparent measurement of the spectral dimension $d_s = 2d_f/d_w$ was larger for FC in the growing cluster ensemble. Since the search algorithm is repeated to obtain an IFC cluster, the effect will be even larger in IFC than in FC percolation, as well as it is larger in FC than in ordinary percolation. Though these effects may simply be a numerical artifact, they might also be genuine, reflecting statistical differences in the static and kinetic ensembles.

5. SUMMARY

In summary, we have introduced and studied an extension to ordinary site percolation on a square lattice which we call *iterated fully coordinated percolation*. The static and dynamic critical behaviors of this model, as well as that of the ordinary and *fully coordinated* percolation models, were determined using methods such as Monte Carlo simulations, finite-size scaling, and normal mode analyses. All clusters used in our simulations were generated statically in grids of predetermined sizes on a square lattice, as opposed to growing them kinetically from a seed according to a rule. We found that the sizes of subregions of full connectivities in an incipient infinite cluster greatly increases as we simulate from ordinary to fully

coordinated and then to iterated fully coordinated percolation. The length scales of such subregions increase by a factor of two to three with each iteration. Although this implies a large increase in the local connectivities, our results also indicate that the ordinary, fully coordinated, and iterated fully coordinated percolation models have identical static and dynamic critical exponents within our statistical errors and thus we believe that they belong to the same universality class, both statically and dynamically.

ACKNOWLEDGMENTS

We are grateful to the Purdue Research Foundation for partial support of this research through a SIRG-PRF Fellowship and to I. Szleifer for informative discussions on related problems in surface kinetics and adsorbate aggregation.

REFERENCES

1. D. Stauffer and A. Aharony, *Introduction to Percolation Theory*, revised 2nd ed. (Taylor and Francis, London, 1994).
2. E. Cuansing, J. H. Kim, and H. Nakanishi, *Phys. Rev. E* **60**:3670 (1999).
3. J. Adler, *Physica A* **171**:453 (1991).
4. P. M. Kogut and P. L. Leath, *J. Phys. C: Solid State Phys.* **15**:4225 (1982).
5. H. E. Stanley and J. Teixeira, *J. Chem. Phys.* **73**:3404 (1980); R. L. Blumberg, G. Shlifer, and H. E. Stanley, *J. Phys. A* **13**:L147 (1980), and references therein.
6. D. Andreica, A. Amato, F. Gygax, M. Pinkpank, and A. Schenck, *Physica B* **289–290**:24 (2000).
7. R. Lenormand and C. Zarcone, in *Kinetics of Aggregation and Gelation*, F. Family and D. P. Landau, eds. (Elsevier, Amsterdam, 1984).
8. J. Adler, R. G. Palmer, and H. Meyer, *Phys. Rev. Lett.* **58**;882 (1987).
9. J. Adler and A. Aharony, *J. Phys. A* **21**:1387 (1988).
10. A. P. Murani and A. Stunault, *Phys. Rev. B* **55**:12518 (1997).
11. For example, surface kinetics which includes discussion of reaction/desorption based on local environments, see M. Silverberg, Ph.D. thesis, Hebrew University, 1987, and references therein.
12. S. Mukherjee and H. Nakanishi, *Fractals* **4**:273 (1996).
13. H. Nakanishi, *Physica A* **196**:33 (1993).
14. J. Hoshen and R. Kopelman, *Phys. Rev. B* **14**:3438 (1976).
15. I. Majid, D. Ben-Avraham, S. Havlin, and H. E. Stanley, *Phys. Rev. B* **30**:1626 (1984).
16. H. Nakanishi, in *Annual Reviews of Computational Physics*, D. Stauffer, ed. (World Scientific, Singapore, 1994), Vol. 1.
17. H. Nakanishi, S. Mukherjee, and N. H. Fuchs, *Phys. Rev. E* **47**:R1463 (1993).
18. S. Alexander and R. Orbach, *J. Phys. Lett.* **43**:L625 (1982).
19. S. Mukherjee, H. Nakanishi, and N. H. Fuchs, *Phys. Rev. E* **49**:5032 (1994).
20. Y. Saad, *Numerical Methods for Large Eigenvalue Problems* (Manchester University Press, Manchester, 1991).
21. F. Family, T. Vicsek, and P. Meakin, *Phys. Rev. Lett* **55**:641 (1985).
22. H. Muralidhar, D. J. Jacobs, D. Ramkrishna, and H. Nakanishi, *Phys. Rev. A* **43**:6503 (1991).